

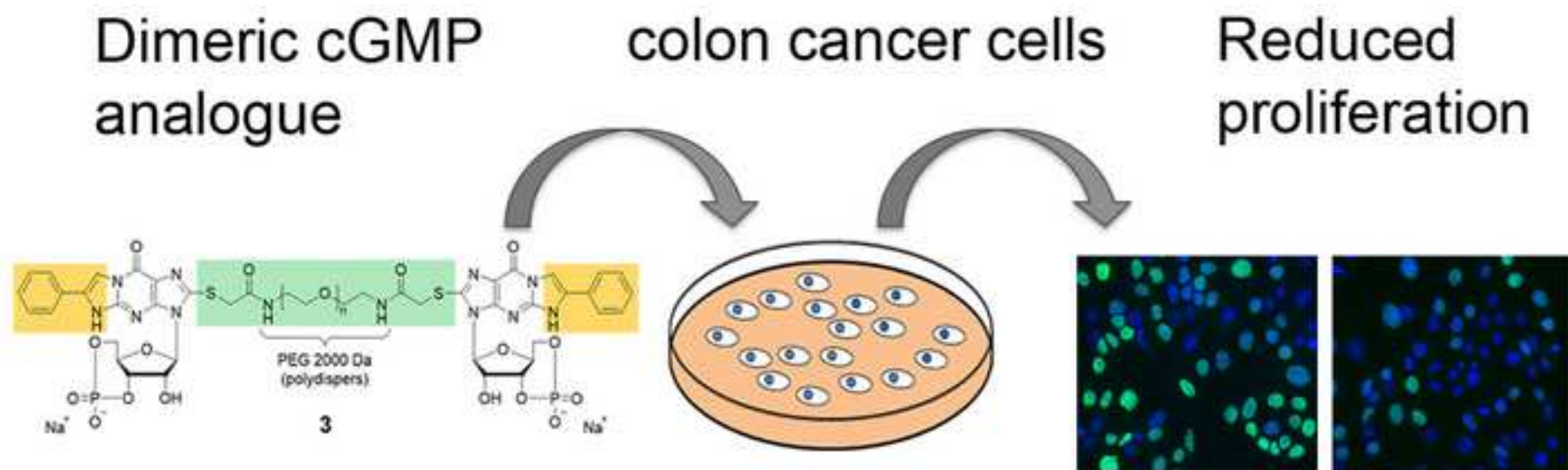
This is the peer reviewed version of the following article:

New dimeric cGMP analogues reduce proliferation in three colon cancer cell lines / Hoffmann, Dorit; Rentsch, Andreas; Vighi, Eleonora; Bertolotti, Evelina; Comitato, Antonella; Schwede, Frank; Genieser, Hans-Gottfried; Marigo, Valeria. - In: EUROPEAN JOURNAL OF MEDICINAL CHEMISTRY. - ISSN 0223-5234. - 141:(2017), pp. 61-72. [10.1016/j.ejmech.2017.09.053]

*Terms of use:*

The terms and conditions for the reuse of this version of the manuscript are specified in the publishing policy. For all terms of use and more information see the publisher's website.

07/01/2026 10:40



## Highlights

- **Three** cGMP analogues linked as dimers were designed and synthesized
- cGMP analogues activate PKG2 in colon cancer cell lines
- Compound 2 had a cytostatic effect on two colon cancer cell lines, i.e. Caco-2 and HCT-116
- Compound 1 reduced cell proliferation and cell survival of HT-29 cells

## **New dimeric cGMP analogues reduce proliferation in three colon cancer cell lines**

Dorit Hoffmann<sup>1</sup>, Andreas Rentsch<sup>2</sup>, Eleonora Vighi<sup>1</sup>, Evelina Bertolotti<sup>1</sup>, **Antonella Comitato<sup>1</sup>**, Frank Schwede<sup>2</sup>, Hans-Gottfried Genieser<sup>2</sup>, Valeria Marigo<sup>1</sup>

<sup>1</sup> Università degli Studi di Modena e Reggio Emilia, Via Campi 287, 41125 Modena, Italy.

<sup>2</sup> BIOLOG Life Science Institute Forschungslabor und Biochemica-Vertrieb GmbH, Flughafendamm 9a, 28199 Bremen, Germany

## Highlights

- **Three** cGMP analogues linked as dimers were designed and synthesized
- cGMP analogues activate PKG2 in colon cancer cell lines
- Compound 2 had a cytostatic effect on two colon cancer cell lines, i.e. Caco-2 and HCT-116
- Compound 1 reduced cell proliferation and cell survival of HT-29 cells

## **Abstract**

Activation of the cGMP-dependent protein kinase G (PKG) can inhibit growth and/or induce apoptosis in colon cancer. In this study we evaluated the effects on cell viability, cell death and proliferation of novel dimeric cGMP analogues, compared to a monomeric compound. Three colon cancer cell lines, which only express isoform 2 of PKG, were treated with these novel cGMP analogues and responded with increased PKG activity. cGMP analogues reduced cell viability in the three cell lines and this was due to a cytostatic rather than cytotoxic effect. These findings suggest that activation of PKG2 can be a therapeutic target in the treatment of colon cancer and, most importantly, that dimeric cGMP analogues can further improve the beneficial effects previously observed with monomeric cGMP analogues.

## **Keywords**

cGMP, Caco-2, HCT 116, HT-29, VASP, PKG2

## 1. Introduction

Colorectal cancer is one of the leading causes of cancer-related mortality in the world with higher prevalence in developed countries [1]. The lower prevalence in developing countries is possibly related to enterotoxigenic *Escherichia coli*, which produces heat-stable enterotoxins (ST). These enterotoxins can mimic the action of endogenous guanylin and uroguanylin by binding to the enzyme guanylyl cyclase (GC) and increasing cGMP levels [2]. Treatments with ST have anti-proliferative effects in colon cancer cell lines [3], [4] suggesting that cGMP signaling can be an important therapeutic target in colon cancer. In fact, several tumor cell lines as well as tumors from human clinical specimens show increased expression of phosphodiesterase 10 (PDE10), leading to hydrolysis of cGMP. The anti-tumor effect of cGMP signaling is further supported by studies using inhibitors of PDE, which increases cGMP concentration, or activators of the cGMP-dependent protein kinase G (PKG). Both of these treatments are able to inhibit growth and to induce apoptosis in some colon cancer cell lines, as does transient expression of constitutively active PKG1 mutants [5]–[8].

PKG is a serine/threonine protein kinase that can be present in the cells in three isoforms (1 $\alpha$ , 1 $\beta$  and 2), encoded by two separate genes, *PRKG1* and *PRKG2*. The *PRKG1* gene can be transcribed from alternative first exons resulting in the two isoforms 1 $\alpha$  and 1 $\beta$ , which differ only in the first ~100 amino acids [9], [10]. An important anti-tumor function for PKG *in vivo* is suggested by a study showing reduced mRNA expression of *PRKG1* in several tumor types, including liver, pancreas and colon. The protein levels of PKG1 were also found reduced in colectomy specimens compared to the normal colon epithelium [11]

One of the downstream targets of PKG is the Vasodilator-stimulated phosphoprotein (VASP), which is involved in the control of mechanical properties of the cytoskeleton. VASP activity is modulated by the phosphorylation at three different sites, Ser157, Ser239 and Thr278. The preferred phosphorylation site of PKG is Ser239 and phosphorylation at this site suppresses the formation of locomotory and invasive actin-based protrusions in colon cancer cell lines [12]. In addition, inhibition of phosphorylation at Ser239 increases survival of colon cancer cell lines while treatment with a PKG activator, that increases phosphorylation at Ser239, reduces assembly of F-actin and promotes cell death [13].

Most colorectal cancers are linked to mutations in adenomatous polyposis coli (*APC*) and  $\beta$ -catenin (*CTNNB1*). Such mutations lead to aberrant activation of the Wnt/ $\beta$ -catenin signaling pathway, nuclear translocation of  $\beta$ -catenin and increased transcription of target genes involved in proliferation and survival [14]. PKG activation in colon cancer cell lines has been linked to decreased expression and nuclear translocation of  $\beta$ -catenin, affecting apoptosis and proliferation [15], [16].

cGMP analogues with good affinity to one or more PKG isoforms and increased resistance to hydrolysis by PDE have been previously reported [17]–[19]. An approach to generate potentially superior analogues was described in a study using a homologous series of a polymer linked dimer (PLD), wherein two cGMP units were tethered via a spacer varied in length. These PLDs showed significantly increased affinity for PKG1 $\alpha$  and a second cellular target, the cyclic-nucleotide-gated (CNG) channels, which depended on the distance between the cGMP units [20]. The strong maximum effect (up to 30 fold for PKG1 $\alpha$  and up to 1000 fold for CNG channels, when compared to monomeric cGMP) was observed at a certain spacer length, unique for each target. Said unique spacer length in turn was suggested to resemble the distance between two binding sites providing increased affinity through



simultaneous occupation of two binding sites. Another reason for the high potency of PLDs could be an increase of the effective concentration as, with one cGMP moiety bound to the target, the diffusion radius of the second one is restricted by the spacer length, potentially leading to a statistically preferred rebinding to the cGMP-binding site of the cGMP-target enzyme.

In this work we examined the effects of an established monomeric cGMP analogue and three new dimeric compounds (PLD) on cell viability, cell death and proliferation in three different colon cancer cell lines. We report data showing that dimers could be more efficient in reducing cell viability when compared to the monomer and thus could be promising compounds for development of new therapies for colon cancer.

## 2. Materials and Methods

### 2.1 Synthesis and activity of new cGMP analogues

#### 2.1.1 General

8- thioguanosine- 3', 5'- cyclic monophosphate (8-T-cGMP) was available from Biolog Life Science Institute (Bremen, Germany), Br-PEG<sub>5</sub>-CH<sub>2</sub>CH<sub>2</sub>Br from BroadPharm (San Diego, USA), NH<sub>2</sub>-PEG<sub>n</sub>-(CH<sub>2</sub>)<sub>2</sub>NH<sub>2</sub> (2000 Da, polydispers) from Iris Biotech (Marktredwitz, Germany), methanol (gradient grade) and acetonitrile (gradient grade) from Honeywell (Seelze, Germany), and ethyl acetate from VWR (Darmstadt, Germany). Other applied solvents and reagents were purchased from Sigma-Aldrich (Darmstadt, Germany). Reverse-phase HPLC chromatography was performed on C18 columns using ODS-A-YMC, 120-S-11 material from YMC Europe (Dinslaken, Germany). Nuclear magnetic resonance (NMR) spectra of compounds (see Supplementary Methods) were recorded for the sodium salt form at 300 K on a 400 MHz Bruker Avance III HD. Chemical shifts are expressed in parts per million (ppm) and were referenced to the solvent residual signal (D<sub>2</sub>O:  $\delta$  = 4.80 ppm) for <sup>1</sup>H spectra. <sup>13</sup>C NMR spectra were referenced to the signal for the methyl group of methanol (10  $\mu$ L, added as an internal standard), which was set to 49.50 ppm. <sup>31</sup>P NMR spectra were referenced to the external standard of 85 % phosphoric acid ( $\delta$  = 0 ppm). All <sup>13</sup>C and <sup>31</sup>P NMR spectra were recorded with proton decoupling.

2.1.2 Preparation of compound 1: Guanosine- 3', 5'- cyclic monophosphate- [8- thio- (pentaethoxy)-ethylthio- 8]- guanosine- 3', 5'- cyclic monophosphate (cGMP-8-T-(EO)<sub>5</sub>-ET-8-cGMP).

*N,N*-diisopropylethylamine (17  $\mu$ L, 102  $\mu$ mol) and Br-PEG<sub>5</sub>-CH<sub>2</sub>CH<sub>2</sub>Br (9 mg, 23  $\mu$ mol)

were added successively to a solution of 8-T-cGMP (triethylammonium salt, 24 mg, 51  $\mu$ mol) in DMSO (400  $\mu$ l). The reaction mixture was stirred for 4 h. The solvent was removed through high vacuum evaporation with a speedvac concentrator. The residue was dissolved in water (1 ml), washed with ethyl acetate (3 x), subjected to preparative reversed phase HPLC and desalted. Yield (Purity): 13  $\mu$ mol, 60% (> 99% HPLC). HPLC: (30% MeOH, 10 mM TEAF buffer, pH 6.8). UV-VIS:  $\lambda_{\text{max}}$  = 274 nm (pH 7),  $\epsilon$  = 24660 (est.).  $^1\text{H}$  NMR (400 MHz,  $\text{D}_2\text{O}$  + 10  $\mu$ L MeOH)  $\delta$  6.05 (s, 2H), 5.29 (ddd,  $J$  = 9.6, 5.5, 1.9 Hz, 2H), 4.95 (d,  $J$  = 5.7 Hz, 2H), 4.48 (ddd,  $J$  = 21.5, 9.3, 4.3 Hz, 2H), 4.34 – 4.25 (m, 2H), 4.18 (td,  $J$  = 10.1, 4.4 Hz, 2H), 3.87 – 3.75 (m, 4H), 3.71 – 3.58 (m, 16H), 3.36 – 3.31 (m, 4H).  $^{13}\text{C}\{^1\text{H}\}$  NMR (100 MHz,  $\text{D}_2\text{O}$  + 10  $\mu$ L MeOH)  $\delta$  158.2, 154.0, 153.2, 145.5, 117.2, 92.9, 77.5 (d,  $J$  = 4.2 Hz), 72.5 (d,  $J$  = 4.1 Hz), 71.8 (d,  $J$  = 8.1 Hz), 70.3, 70.3, 70.1, 69.8, 67.9 (d,  $J$  = 6.8 Hz), 34.2.  $^{31}\text{P}\{^1\text{H}\}$  NMR (162 MHz,  $\text{D}_2\text{O}$  + 10  $\mu$ L MeOH)  $\delta$  -0.81. ESI-MS (+):  $m/z$  calculated for  $\text{C}_{32}\text{H}_{46}\text{N}_{10}\text{O}_{19}\text{P}_2\text{S}_2\text{Na}$  ( $[\text{M}+\text{Na}]^+$ ): 1023.18, found: 1023. ESI-MS (-):  $m/z$  calculated for  $\text{C}_{32}\text{H}_{45}\text{N}_{10}\text{O}_{19}\text{P}_2\text{S}_2$  ( $[\text{M}-\text{H}]^-$ ): 999.18, found: 999.

2.1.3 Preparation of compound 2: Guanosine- 3', 5'-cyclic monophosphate- [8-thiomethylamido- (PEG pd 2000)-amidomethylthio- 8]- guanosine- 3', 5'-cyclic monophosphate (cGMP-8-TMAmd-(PEG pd 2000)-AmdMT-8-cGMP).

*N,N*-diisopropylethylamine (16  $\mu$ l, 96  $\mu$ mol) and PyBOP<sup>®</sup> (26 mg, 50  $\mu$ mol) were added successively to a solution of 8- carboxymethylthioguanosine- 3', 5'- cyclic monophosphate (8-CMT-cGMP, triethyl ammonium salt, 25 mg, 46  $\mu$ mol) (see supplementary information) and  $\text{NH}_2\text{-PEG}_n\text{-(CH}_2\text{)}_2\text{NH}_2$  (2000 Da, polydispers, 44.7 mg, 23  $\mu$ mol) in DMSO (700  $\mu$ l). The reaction mixture was stirred for 15 min. Water (100  $\mu$ l) was added, stirring was continued for 10 min and the solvent was removed through high vacuum evaporation with a speedvac concentrator. The residue was dissolved in water (1 ml), the pH was adjusted to 6 and the solution

washed with ethyl acetate (5 x). The aqueous phase was evaporated under reduced pressure using a rotary evaporator, redissolved in water, subjected to preparative reversed phase HPLC and desalted, giving the title compound. Yield (Purity): 10.8  $\mu$ mol, 47 % (> 99% HPLC). HPLC: (Gradient, 21% then 24% MeCN, 50 mM NaH<sub>2</sub>PO<sub>4</sub> buffer, pH 6.8). UV-VIS:  $\lambda_{\text{max}}$  = 275 nm (pH 7),  $\epsilon$  = 24660 (est.). <sup>1</sup>H NMR (400 MHz, D<sub>2</sub>O + 10  $\mu$ L MeOH)  $\delta$  6.04 (s, 2H), 5.31 (ddd,  $J$  = 9.8, 5.7, 2.1 Hz, 2H), 4.92 (d,  $J$  = 5.7 Hz, 2H), 4.51 (ddd,  $J$  = 21.4, 9.3, 4.6 Hz, 2H), 4.36 – 4.27 (m, 2H), 4.22 (td,  $J$  = 10.1, 4.6 Hz, 2H), 3.92 – 3.90 (m, 4H), 3.83 – 3.52 (m, 184H), 3.44 – 3.38 (m, 4H). <sup>13</sup>C{<sup>1</sup>H} NMR (100 MHz, D<sub>2</sub>O + 10  $\mu$ L MeOH)  $\delta$  170.8, 158.2, 154.1, 153.4, 144.0, 117.4, 92.9, 77.5 (d,  $J$  = 4.1 Hz), 72.6 (d,  $J$  = 4.0 Hz), 72.0 (d,  $J$  = 8.2 Hz), 70.2, 70.0, 69.3, 67.8 (d,  $J$  = 7.1 Hz), 40.1, 37.4. <sup>31</sup>P{<sup>1</sup>H} NMR (162 MHz, D<sub>2</sub>O + 10  $\mu$ L MeOH)  $\delta$  -0.97. ESI-MS (-):  $m/z$  calculated for C<sub>114</sub>H<sub>206</sub>N<sub>12</sub>O<sub>60</sub>P<sub>2</sub>S<sub>2</sub> ( $n$  = 44, [M-2H]<sup>2-</sup>): 1414.62, found: 1414.

2.1.4 Preparation of compound 3:  $\beta$ - Phenyl- 1, N<sup>2</sup>-ethenoguanosine- 3', 5'-cyclic monophosphate- [8- thiomethylamido- (PEG pd 2000)- amidomethylthio- 8]-  $\beta$ - phenyl- 1, N<sup>2</sup>-ethenoguanosine- 3', 5'-cyclic monophosphate (PET-cGMP-8-TMAmd- (PEG pd 2000)-AmdMT-8-cGMP-PET).

Using the procedure described for compound 2, 8- Carboxymethylthio-  $\beta$ - phenyl- 1, N<sup>2</sup>- ethenoguanosine- 3', 5'- cyclic monophosphate (8-CMT-PET-cGMP, triethyl ammonium salt, 22 mg, 36  $\mu$ mol) (see supplementary information) was reacted with NH<sub>2</sub>-PEG<sub>*n*</sub>-(CH<sub>2</sub>)<sub>2</sub>NH<sub>2</sub> (2000 Da, polydispers). More PyBOP (0.5 eq) was added stepwise to drive the reaction to completion and yield the title compound. Yield (Purity): 35% (> 99% HPLC). HPLC: (28% MeCN, 25 mM NaH<sub>2</sub>PO<sub>4</sub> buffer, pH 6.8). UV-VIS:  $\lambda_{\text{max}}$  = 272 nm (pH 7),  $\epsilon$  = 72000 (est.). <sup>1</sup>H NMR (400 MHz, D<sub>2</sub>O + 10  $\mu$ L MeOH)  $\delta$  7.37 (s, 2H), 7.19 – 7.08 (m, 4H), 7.04 – 6.91 (m, 4H), 6.86 – 6.69 (m, 2H), 5.84 (s, 2H), 5.50 – 5.39 (m, 2H), 4.64 – 4.50 (m, 2H), 4.42 – 4.31 (m, 2H), 4.29 –

4.19 (m, 2H), 3.95 – 3.84 (m, 4H), 3.83 – 3.49 (m, 195H), 3.47 – 3.41 (m, 4H). Note: As confirmed by COSY NMR, the ribose H2' shows the same chemical shift as the solvent residual signal (4.80 ppm).  $^{13}\text{C}\{^1\text{H}\}$  NMR (100 MHz,  $\text{D}_2\text{O}$  + 10  $\mu\text{L}$  MeOH)  $\delta$  170.5, 151.2, 150.8, 145.6, 144.8, 130.1, 129.0, 128.8, 125.9, 123.9, 116.3, 102.3, 92.5, 77.6, 72.5, 71.9, 70.2, 70.0, 69.3, 68.0, 40.1, 36.7.  $^{31}\text{P}\{^1\text{H}\}$  NMR (162 MHz,  $\text{D}_2\text{O}$ )  $\delta$  -0.76. ESI-MS (-):  $m/z$  calculated for  $\text{C}_{130}\text{H}_{214}\text{N}_{12}\text{O}_{60}\text{P}_2\text{S}_2$  ( $n=44$ ,  $[\text{M}-2\text{H}]^{2-}$ ): 1516.16, found: 1516.

## 2.2 Cell culture

The Caco-2 (ATCC<sup>®</sup> HTB-37<sup>™</sup>), HCT 116 (ATCC<sup>®</sup> CCL-247<sup>™</sup>), and HT-29 (ATCC<sup>®</sup> HTB-38<sup>™</sup>) human colon cancer cell lines were grown in DMEM (Dulbecco's Modified Eagle Medium) high glucose medium (4.5 mg/ml) supplemented with 10% Fetal bovine serum (FBS), 2 mM Glutamine, 100 U/ml penicillin, and 100  $\mu\text{g}/\text{ml}$  streptomycin purchased from Invitrogen (ThermoFisher Scientific, Monza, Italy). Cells were kept at 37°C in a humidified atmosphere of 5%  $\text{CO}_2$  and subcultured every 2-3 days. For treatment, cells were plated in 24-well or 96-well plates, depending on the experiment, and after 8 h the medium was changed to serum-free medium. After additional 12 h (HCT 116) or 36 h (Caco-2 and HT-29), the cells were incubated in serum-free medium containing the test compounds at different concentrations for 24 h.

## 2.3 RNA Interference (RNAi)

A sequence beginning with an AA dinucleotide was chosen in the PKG2 mRNA, and we designed hairpin RNAi template oligonucleotides (shRNA). The control shRNA was generated from a scrambled sequence not targeting any known gene. The sequences (5'→3') are as following: PKG2 AAGTGAATACTATGACAAAG, scrambled GCATACTACCACTAGAGTTTA.

Retroviruses from pSUPER.retro.puro vector (OligoEngine, Seattle, WA, USA), expressing the shRNAs, were prepared by transient transfection in amphotropic Phoenix-AMPHO packaging cells (ATCC, Rockville, MD, USA). Caco-2 cells were infected with either shRNA or scramble expressing retroviruses and selected with puromycin (1 µg/ml). The acquired stable clones were called Caco-2 shRNA PKG2 and Caco-2 scrambled and the effect on PKG2 expression was assessed by immunoblotting using an anti-PKG2 antibody.

#### 2.4 Western Blot analysis

For protein extraction, cells were harvested at 70-90% confluence, pelleted and resuspended in RIPA lysis buffer (50 mM Tris-HCl (pH 7.5), 150 mM NaCl, 1 mM EDTA, 1% NP-40, 0.1% w/v SDS, 1 mM Na<sub>3</sub>VO<sub>4</sub>, 1 mM NaPO<sub>4</sub>, 1X protease inhibitor cocktail from Sigma, Milan, Italy). The cells were incubated for 1 h at 4°C in rotation, cell debris and chromatin were eliminated by centrifugation and protein concentration was determined by Bradford assay (Bio-Rad, Segrate, Italy).

Proteins were separated using SDS-PAGE and transferred to PVDF membrane (Amersham, Milan, Italy). The membranes were blocked in 5% BSA for PKG1α, PKG1β and pVASP or 5% milk for PKG2 and actin in phosphate-buffered saline (PBS) and 0.1% Tween for 1 h at room temperature and incubated overnight at 4°C with the primary antibodies for PKG1α, PKG1β, PKG2 (1:1000; Santa Cruz Biotechnology, Heidelberg, Germany), pVASP (1:2000; Sigma) and actin (1:2000; Sigma). As secondary antibodies horseradish peroxidase-conjugated anti-rabbit, anti-mouse (Amersham) or anti-goat (Santa Cruz Biotechnologies) were incubated for 1 h at room temperature. Protein bands were visualized using the Femto kit (Euroclone, Pero, Italy) for PKG1α and PKG1β, the Clarity kit (Bio-Rad) for PKG2 and pVASP and the Pico kit (Euroclone) for actin.

## 2.5 Cell viability assay

Cell viability was determined using the colorimetric MTT (3-(4,5 dimethylthiazol-2-yl)-2,5-diphenyltetrazolium bromide) assay. Cells were seeded in 96-well culture plates at  $3 \times 10^3$  (Caco-2, **Caco-2 shRNA PKG2**, **Caco-2 scrambled** and HT-29) and  $5 \times 10^3$  (HCT 116) cells/well. After the treatment, the medium was removed and the cells were incubated with 50  $\mu$ l MTT (Sigma) at the concentration of 1 mg/ml for 90 min at 37°C. The supernatant was removed and isopropanol (100  $\mu$ l/well) was added. The purple formazan crystals were dissolved by shaking the plates for 10 min on a tumbling table and the absorbance was measured at 570 nm with a microplate reader (Labsystems Multiskan MCC/340, ThermoFisher Scientific). In each experiment the values of not treated cells were set to 100% cell viability.

## 2.6 Immunofluorescence

$2 \times 10^4$  cells/well were seeded on coverslips in 24-well plates. The medium was changed to serum-free medium 8 h later. They were kept in serum-free medium for additional 12 h (HCT 116) or 36 h (Caco-2 and HT-29).

For immunofluorescence staining of PKG2, the cells were washed in PBS and fixed in 4% paraformaldehyde (PFA) for 10 min at room temperature. For immunofluorescence of phosphorylated VASP and  $\beta$ -catenin, the cells were washed in PBS and fixed in 4% PFA for 10 min at room temperature after incubation for 24 h with the test compounds.

Cells were blocked for 45 min in blocking buffer (3% BSA, 0.2% Triton-X100 in PBS for PKG2; 3% BSA, 0.2% Tween20 in Tris-Buffered Saline for pVASP) and then incubated overnight with primary antibodies. For  $\beta$ -catenin staining, cells were permeabilized with 0.1% sodium citrate and 0.1% Triton-X100 in PBS for 2 min,

blocked for 15 min with 1% BSA in PBS and then incubated with the primary antibody for 3 h.

As primary antibodies we used: rabbit anti-PKG2 (1:100; Santa Cruz Biotechnologies), mouse anti-pVASP at Ser239 (1:200; Nanotools, Antikörpertechnik, Teningen, Germany) and mouse anti- $\beta$ -catenin (1:500; BD Biosciences). Slides were then washed in PBS and incubated for 45 min with 0.1  $\mu$ g/ml 4', 6-diamidino-2-phenylindole (DAPI, Sigma) and anti-mouse Alexa Fluor 568 or anti-rabbit Alexa Fluor 568 secondary antibodies (1:1000; Molecular Probes, Monza, IT) and, after extensive washes with PBS, finally mounted with Mowiol 4-88 (Sigma). Images were taken using an Axioplan microscope (Zeiss, Arese, Italy).

## 2.7 Cell death assay

$2 \times 10^4$  cells/well were seeded on cover glasses in 24-well plates. After treatment with the compounds, the medium was removed and cells were washed with PBS and fixed in 4% PFA in PBS for 10 min at room temperature. Cells were incubated with 2 mM Ethidium Homodimer (ThermoFisher Scientific) for 2 min, followed by counterstaining with 0.1  $\mu$ g/ml DAPI (Sigma) for 2 min. After washes with PBS, slides were mounted with Mowiol 4-88 (Sigma), images were taken using an Axioplan microscope (Zeiss). Ethidium Homodimer stained and DAPI stained nuclei cells were counted. The percentage of dying cells was expressed as the ratio of Ethidium Homodimer positive cells over the total number of cells (DAPI<sup>+</sup>).

## 2.8 Proliferation assay

Cell proliferation was determined by bromodeoxyuridine (BrdU, Sigma) incorporation analysis, as previously published [21]. Briefly,  $2 \times 10^4$  cells/well were seeded on cover glasses in 24-well plates. After treatment with the compounds, cells were incubated for 90 min in serum-free medium containing 1  $\mu$ M BrdU (Sigma). Cells were washed with PBS and fixed in 4% PFA for 10 min at room temperature and incubated with 2N



HCl for 30 min at 37°C. After incubation at room temperature with 0.1 M borate buffer pH 8.5 for 15 min, slides were washed with PBS and blocked with 5% BSA and 0.3% Triton-X100 in PBS for 1 h at room temperature. Cells were then incubated overnight with mouse-anti-BrdU (1:100; Developmental Hybridoma, Iowa City, USA) and, after extensive washes with PBS, incubated with anti-mouse Oregon Green antibody (1:1000; ThermoFisher Scientific) and 0.1 µg/ml DAPI for 1 h. After washes with PBS, slides were mounted with Mowiol 4-88 (Sigma) and images were taken using an Axioplan microscope (Zeiss). BrdU labeled cells were counted using the ImageJ software. The percentage of proliferating cells was expressed as the ratio of BrdU positive cells over the total number of cells (DAPI<sup>+</sup>). In each experiment the values of not treated cells was set to 100% cell proliferation.

## 2.9 Statistical analysis

All experiments were repeated in at least three independent experiments. The results were expressed as mean ± standard deviation (SD). Statistical analysis was performed by comparing treated and not treated samples with the unpaired Student's t-test and a P value ≤0.05 was considered significant (\*≤0.05, \*\*≤0.01, \*\*\*≤0.001).

### 3. Results and discussion

#### 3.1 Expression of PKG isoforms in the Caco-2, HT-29 and HCT 116 cell line

Reduced protein levels of PKG1 can be found in different tumor types [22], and the expression of the 2 isoforms in established cancer cell lines remains controversial and studies often rely on overexpression of PKG1 [5], [23], [24]. Expression of PKG2 is also not well characterized in the cell lines used in this work. We thus analyzed protein levels of PKG1 $\alpha$ , PKG1 $\beta$  and PKG2. We could detect only PKG2 by immunoblotting and PKG1 $\alpha$  and PKG1 $\beta$  were undetectable in the three cell lines (Fig. 1A). Immunofluorescence analysis confirmed expression with an intracellular localization of PKG2 in the three cell lines (Fig. 1B).

#### 3.2 Synthesis of new cGMP analogues

Seeking to transfer the reported high activating potency of polymer linked dimeric cGMP (PLD) analogues [20] to further targets of the cGMP signal transduction cascade, in particular PKG2, being the expressed PKG isoform within the three studied cancer cell lines, three new PLD analogues were synthesized. Therein, in accordance to Kramer and Karpen [20], we kept linkage via a thio-function at the 8-position of the nucleobase (Fig. 2) and introduced polyethylene glycol (PEG) spacers of different lengths with compound 1 featuring the shortest (5 ethylene oxide units) and compound 2 and 3 having a larger spacer (both polydispers spacers with an average molecular weight of 2000 Da corresponding to an average of 45 ethylene oxide units). The reported synthetic strategy applied coupling of 8-T-cGMP with vinyl sulfonyl substituted PEG (spacer) reagents, giving additional sulfonyl bridging functions. However, it also generates a regioselectivity issue as the N7-position is

also reactive under these conditions [25]. We therefore replaced the published protocol in favor of more regioselective methods. These contained a halide displacement reaction (compound 1) and amide bond formation (compound 2 and 3). Compound 3, which apart from that is identical to compound 2, was further modified at the nucleobase by attachment of a  $\beta$ -phenyl-1,N<sup>2</sup>-etheno (PET) group. As monomeric reference we selected 8-Br-PET-cGMP, a synthetic precursor of compound 3 and established PKG2 activator [18].

### 3.3 Increased phosphorylation of VASP after treatment with PKG activators

The three colon cancer cell lines were treated with 8-Br-PET-cGMP, compound 1, compound 2 and compound 3. To assess their ability to increase PKG activity, phosphorylation of VASP at the residue Serine 239 (pVASP) was examined. Serine 239 is preferentially phosphorylated by PKG and can be used as an indicator of increased PKG activity [26]. Immunofluorescence analyses for pVASP in Caco-2 cells demonstrated an increased pVASP staining after treatment with 10  $\mu$ M 8-Br-PET-cGMP as well as all three compounds compared to untreated cells (Fig. 3A-E). Immunoblotting confirmed the increased level of pVASP after treatment with 8-Br-PET-cGMP and compound 1, 2 and 3 (Fig. 3P). In HT-29 cells increased pVASP immunofluorescence could be observed after treatment with 8-Br-PET-cGMP (Fig. 3G) and compound 1 (Fig. 3H) when compared to untreated cells (Fig. 3F). Immunoblotting confirmed the increased levels of pVASP after treatment with 8-Br-PET-cGMP and compound 1 but also showed increased pVASP levels with compound 2 and 3 (Fig. 3Q). In HCT 116 cells increased pVASP immunofluorescence could be observed after treatment with compound 1 (Fig. 3M) and compound 2 (Fig. 3N) when compared to untreated cells (Fig. 3K). A strong

increase in pVASP could also be confirmed by immunoblotting after treatment with compound 1 compound 2 (Fig. 3R).

These compounds were then used at different concentrations to examine possible changes in cell viability, cell death and proliferation as a result of increased PKG activity.

3.4 Treatment with PKG activators decreased cell viability by decreasing proliferation and/or increasing cell death in the Caco-2, HT-29 and HCT 116 cell lines

The three cell lines were treated with the cGMP analogs at concentrations from 1 nM to 10  $\mu$ M and cell viability was assessed using the MTT assay. A significant decrease in cell viability was observed in the Caco-2 cell line after treatment with 8-Br-PET-cGMP, compound 2 and compound 3 compared to not treated (nt) cells, with compound 2 having the strongest effect (Fig. 4A). At the lowest concentration (1nM), treatment with compound 2 also significantly reduced cell viability when compared to 8-Br-PET-cGMP at its best concentration (100 nM). Compound 2 reduced cell proliferation, as assessed by BrdU assay, (Fig. 4B) but did not significantly increase cell death (Fig. 4C), suggesting that the compounds do not exert a cytotoxic effect. We found a strong correlation by comparing cell viability and cell proliferation (Fig. 4D) suggesting a cytostatic effect of compound 2 on Caco-2 cells.

Treatments with compound 1 (100 nM to 10  $\mu$ M) and with 8-Br-PET-cGMP at the highest concentration (10  $\mu$ M) caused a significant decrease in cell viability of the HT-29 cell line (Fig. 5A). A trend towards decreased viability after treatment with compound 2 and compound 3 could also be observed, but without statistically significant results. These two compounds also had increased pVASP levels, as shown in Fig, 3Q, but unlike 8-Br-PET-cGMP and compound 1 did not decrease cell

viability at 10  $\mu$ M. It is possible that additional, unknown targets are affected by the treatment with these analogues at high concentrations, possibly masking an effect on cell viability. Compound 1 reduced cell proliferation and increased cell death (Fig. 5B). Quantifications of these results showed a significant, even if small, cytotoxic effect from 100 nM to 10  $\mu$ M (Fig. 5C). By comparing cell viability and cell proliferation we found a significant reduction in proliferation after treatment with 8-Br-PET-cGMP at 10  $\mu$ M and, interestingly, compound 1 showed a high cytostatic effect starting from 10 nM (Fig. 5D).

When we analyzed the effects of the compounds in the HCT 116 cell line we found a significant decrease in cell viability after treatment with compound 1 and compound 2, with compound 2 having the strongest effect (Fig. 6A). Compound 3, on the other hand, increased cell viability in the HCT 116 cell line. Compound 2 reduced cell proliferation (Fig. 6B) but did not induce cell death (Fig. 6C), suggesting no cytotoxic effect. By comparing cell viability and cell proliferation we found a significant reduction in proliferation after treatment with compound 2 at all tested concentrations, correlating decreased cell viability with a cytostatic effect (Fig. 6D).

Interestingly, compound 3 decreased cell viability only in the Caco-2 cell line but not in the other two tested cell lines. This compound, in fact, could strongly activate PKG, as defined by VASP phosphorylation, only in Caco-2 cells. The different effects of the compounds in the activation of PKG and on cell viability cannot be explained by differential expression of the different PKG isoforms, as these cells express only PKG2, and we can only speculate that other, not yet identified, targets, differentially expressed by Caco-2, may contribute to these differences.

To define possible toxic effects of the new cGMP analogs in non-tumor cells, we treated Cos7 cells with 8-Br-PET-cGMP, compound 1 and compound 2 and we did not observe any decrease in cell viability (data not shown).

### 3.5 Treatment with PLD compound 2 reduced nuclear localization of $\beta$ -catenin in the Caco-2 cell line

The Caco-2 cell line is known to exhibit nuclear localization of  $\beta$ -catenin. The Caco-2 cell line contains both a *CTNNB1* mutation (missense mutation in codon 245) and an *APC* mutation (truncation at position 1367), while HT-29 and HCT 116 only contain one of the mutations, either in the *APC* gene (HT-29) or the *CTNNB1* gene (HCT 116) [27], [28]. HT-29 and HCT 116 cells show little to no nuclear localization and stimulation with Wnt3a is needed to induce/increase nuclear localization of  $\beta$ -catenin [16], [29]–[31]. We therefore chose the Caco-2 cell line to assess possible changes in  $\beta$ -catenin subcellular localization after treatment with a cGMP dimeric analogue, specifically compound 2. Nuclear localization of  $\beta$ -catenin can be observed in most not treated cells (Fig. 7A, arrows). After treatment with compound 2 at its best concentration (100 nM),  $\beta$ -catenin was less localized to the nuclei (Fig. 7B, empty arrows), suggesting that increased PKG2 activity reduced nuclear translocation of  $\beta$ -catenin in the Caco-2 cell line.

The substantial reduction of nuclear localization of  $\beta$ -catenin in the Caco-2 cells after treatment with compound 2, suggests that increased PKG2 activity might contribute to the observed decrease in proliferation by restraining  $\beta$ -catenin activation. We cannot exclude that  $\beta$ -catenin might contribute in reducing proliferation in the HT-29 and HCT 116 cells under these conditions. In our study, we showed that PKG2

activation inhibited growth in all tested colon cancer cell lines possibly by interfering with  $\beta$ -catenin activation but it is possible that additional mechanism(s) are activated by PKG2 [32]. One of these pathways may involve VASP phosphorylation at Serine 239 that we demonstrated after treatment with the compounds. In fact, a direct correlation of VASP phosphorylation with colon cancer viability was recently reported [13]. Another mechanism might be linked to the activation of tumor suppressors of the FoxO family as previously found in different colon cancer cell lines [33]–[35].

### 3.6 The effects of compound 2 on Caco-2 cell viability is mediated by PKG2

To assess the role of PKG2 in the decrease of cell viability after treatment with cGMP analogues, we downregulated *PKG2* expression using shRNA targeting *PKG2* mRNA in Caco-2 cells. As shown in Fig. 8A, expression of PKG2 was reduced to around 18% compared to the endogenous expression in Caco-2 or in Caco-2 scrambled cells (negative control, see methods). Downregulated cells were then treated with compound 2 at concentrations from 1 nM to 10  $\mu$ M and cell viability was assessed using the MTT assay. Caco-2 and Caco-2 scrambled showed a similar reduction in cell viability after treatment (Fig. 8B), whereas the effect of compound 2 was lost in Caco-2 shRNA PKG2 cells, suggesting that PKG2 plays an important role in the observed reduction in cell viability after treatment with compound 2.

## Conclusions

This study presents three novel cGMP analogues, in the form of dimers with PEG linkers, and their effects in three colorectal cancer cell lines. We report that treatment with different cGMP analogues led to a significant reduction of cell viability. In the Caco-2 and HCT 116 cell lines the dimeric compound 2 generated the best result, in the HT-29 cell line the best result was obtained with compound 1. In all cases the results with these dimeric compounds were more pronounced than with the monomeric 8-Br-PET-cGMP. The results from the Ethidium Homodimer and BrdU assays suggested that the reduction in cell viability was mainly due to reduced proliferation and a cytotoxic effect was observed only with compound 1 in HT-29 cells. Downregulation of PKG2 in the Caco-2 cell line abolished the effect of compound 2, strongly suggesting that the reduction of cell viability was mediated by PKG2 activity.

Taken together these results suggest that activation of PKG2 could be a therapeutic target in the treatment of colon cancer by reducing proliferation. Most importantly, dimeric cGMP analogues are cell permeable and can improve the beneficial effects that have been observed using monomeric cGMP analogues.



## **Acknowledgements**

We acknowledge the CIGS (Cinzia Restani) for providing confocal microscopy assistance as well as the Cell-lab facility at University of Modena and Reggio Emilia. We thank Dr S. Alboni and C. Benatti for technical help. This work was supported by the European Union (DRUGSFORD; HEALTH-F2-2012-304963).

## **Author contribution**

AR, FS, HGG designed and performed cGMP analogue synthesis; DH, EV and EB performed the experiments and analysed the data; AC generated shRNA PKG2 constructs and viruses; VM designed the experiments and analysed the data; DH and VM drafted the manuscript; DH, EV, EB, AR, FS, HGG and VM revised the manuscript and approved the final version submitted.

## **Declaration of Interest**

Hans-Gottfried Genieser is CEO, Frank Schwede and Andreas Rentsch are employees of Biolog Life Science Institute, which is selling 8-Br-PET-cGMP as research reagent.

## Bibliography

- [1] “WHO | World Cancer Report 2014,” *WHO*, (2015).
- [2] S. Uzzau and A. Fasano “Cross-talk between enteric pathogens and the intestine” *Cell. Microbiol.* 2 (2000) 83–89.
- [3] S. Kazerounian, G. M. Pitari, F. J. Shah, G. S. Frick, M. Madesh, I. Ruiz-Stewart, S. Schulz, G. Hajnóczy, and S. A. Waldman “Proliferative signaling by store-operated calcium channels opposes colon cancer cell cytostasis induced by bacterial enterotoxins” *J. Pharmacol. Exp. Ther.* 314 (2005) 1013–1022.
- [4] G. M. Pitari, L. V Zingman, D. M. Hodgson, A. E. Alekseev, S. Kazerounian, M. Bienengraeber, G. Hajnoczky, A. Terzic, and S. A. Waldman “Bacterial enterotoxins are associated with resistance to colon cancer” *Proc Natl Acad Sci U S A* 100 (2003) 2695–2699.
- [5] A. Deguchi, S. W. Xing, I. Shureiqi, P. Yang, R. A. Newman, S. M. Lippman, S. J. Feinmark, B. Oehlen, and I. B. Weinstein “Activation of protein kinase G up-regulates expression of 15-lipoxygenase-1 in human colon cancer cells” *Cancer Res.* 65 (2005) 8442–8447.
- [6] B. Zhu, L. Vemavarapu, W. J. Thompson, and S. J. Strada “Suppression of cyclic GMP-specific phosphodiesterase 5 promotes apoptosis and inhibits growth in HT29 cells” *J. Cell. Biochem.* 94 (2005) 336–350.
- [7] M. C.-T. Hu, D.-F. Lee, W. Xia, L. S. Golfman, F. Ou-Yang, J.-Y. Yang, Y. Zou, S. Bao, N. Hanada, H. Saso, R. Kobayashi, and M.-C. Hung “I $\kappa$ B Kinase Promotes Tumorigenesis through Inhibition of Forkhead FOXO3a” *Cell* 117

(2004) 225–237.

- [8] N. Li, K. Lee, Y. Xi, B. Zhu, B. D. Gary, V. Ramírez-Alcántara, E. Gurpinar, J. C. Canzoneri, A. Fajardo, S. Sigler, J. T. Piazza, X. Chen, J. Andrews, M. Thomas, W. Lu, Y. Li, D. J. Laan, M. P. Moyer, S. Russo, B. T. Eberhardt, L. Yet, A. B. Keeton, W. E. Grizzle, and G. A. Piazza “Phosphodiesterase 10A: a novel target for selective inhibition of colon tumor cell growth and  $\beta$ -catenin-dependent TCF transcriptional activity” *Oncogene* 34 (2015) 1499–1509.
- [9] S. Orstavik, V. Natarajan, K. Taskén, T. Jahnsen, and M. Sandberg “Characterization of the human gene encoding the type I alpha and type I beta cGMP-dependent protein kinase (PRKG1)” *Genomics* 42 (1997) 311–318.
- [10] S. Orstavik, R. Solberg, K. Taskén, M. Nordahl, M. R. Altherr, V. Hansson, T. Jahnsen, and M. Sandberg “Molecular cloning, cDNA structure, and chromosomal localization of the human type II cGMP-dependent protein kinase” *Biochem. Biophys. Res. Commun.* 220 (1996) 759–765.
- [11] Y. Hou, N. Gupta, P. Schoenlein, E. Wong, R. Martindale, V. Ganapathy, and D. Browning “An anti-tumor role for cGMP-dependent protein kinase” *Cancer Lett.* 240 (2006) 60–68.
- [12] D. S. Zuzga, J. Pelta-Heller, P. Li, A. Bombonati, S. A. Waldman, and G. M. Pitari “Phosphorylation of vasodilator-stimulated phosphoprotein Ser239 suppresses filopodia and invadopodia in colon cancer” *Int. J. Cancer* 130 (2012) 2539–2548.
- [13] M. Ali, L. K. Rogers, and G. M. Pitari “Serine phosphorylation of vasodilator-stimulated phosphoprotein (VASP) regulates colon cancer cell survival and apoptosis” *Life Sci.* 123 (2015) 1–8.

- [14] M. Masuda, M. Sawa, and T. Yamada "Therapeutic targets in the Wnt signaling pathway: Feasibility of targeting TNIK in colorectal cancer" *Pharmacol. Ther.* 156 (2015) 1–9.
- [15] N. Li, Y. Xi, H. N. Tinsley, E. Gurpinar, B. D. Gary, B. Zhu, Y. Li, X. Chen, A. B. Keeton, A. H. Abadi, M. P. Moyer, W. E. Grizzle, W.-C. Chang, M. L. Clapper, and G. A. Piazza "Sulindac Selectively Inhibits Colon Tumor Cell Growth by Activating the cGMP/PKG Pathway to Suppress Wnt/ $\beta$ -Catenin Signaling.," *Mol. Cancer Ther.* 12 (2013) 1848–1859.
- [16] K. Lee, A. S. Lindsey, N. Li, B. Gary, J. Andrews, B. Adam, and G. A. Piazza " $\beta$ -catenin nuclear translocation in colorectal cancer cells is suppressed by PDE10A inhibition, cGMP elevation, and activation of PKG" *Oncotarget* 7 (2016) 5353–5365.
- [17] F. Schwede, E. Maronde, H. G. Genieser, and B. Jastorff "Cyclic nucleotide analogs as biochemical tools and prospective drugs" *Pharmacology and Therapeutics* 87(2000) 199–226.
- [18] H. Poppe, S. D. Rybalkin, H. Rehmann, T. R. Hinds, X.-B. Tang, A. E. Christensen, F. Schwede, H.-G. Genieser, J. L. Bos, S. O. Doskeland, J. A. Beavo, and E. Butt "Cyclic nucleotide analogs as probes of signaling pathways" *Nat. Methods* 5 (2008) 277–278.
- [19] K. R. Sekhar, R. J. Hatchett, J. B. Shabb, L. Wolfe, S. H. Francis, J. N. Wells, B. Jastorff, E. Butt, M. M. Chakinala, and J. D. Corbin "Relaxation of pig coronary arteries by new and potent cGMP analogs that selectively activate type I alpha, compared with type I beta, cGMP-dependent protein kinase" *Mol. Pharmacol.* 42(1992) 103-108.

- [20] R. H. Kramer and J. W. Karpen "Spanning binding sites on allosteric proteins with polymer-linked ligand dimers" *Nature* 395 (1998) 710–713.
- [21] F. Giordano, A. De Marzo, F. Vetrini, and V. Marigo "Fibroblast growth factor and epidermal growth factor differently affect differentiation of murine retinal stem cells in vitro" *Mol. Vis.* 13 (2007) 1842–1850.
- [22] Y. Hou, E. Wong, J. Martin, P. V. Schoenlein, W. R. Dostmann, and D. D. Browning "A role for cyclic-GMP dependent protein kinase in anoikis" *Cell. Signal.* 18 (2006) 882–888.
- [23] A. Deguchi, W. J. Thompson, and I. B. Weinstein "Activation of Protein Kinase G Is Sufficient to Induce Apoptosis and Inhibit Cell Migration in Colon Cancer Cells" *Cancer Res.* 64 (2004) 3966–3973.
- [24] D. D. Browning, I.-K. Kwon, and R. Wang "cGMP-dependent protein kinases as potential targets for colon cancer prevention and treatment" *Future Med. Chem.* 2 (2010) 65–80.
- [25] T. Strassmaier and J. W. Karpen "Novel N7- and N1-Substituted cGMP Derivatives Are Potent Activators of Cyclic Nucleotide-Gated Channels" *J. Med. Chem.* 50 (2007) 4186–4194.
- [26] A. Smolenski, C. Bachmann, K. Reinhard, P. Honig-Liedl, T. Jarchau, H. Hoschuetzky, and U. Walter "Analysis and Regulation of Vasodilator-stimulated Phosphoprotein Serine 239 Phosphorylation in Vitro and in Intact Cells Using a Phosphospecific Monoclonal Antibody" *J. Biol. Chem.* 273 (1998) 20029–20035.
- [27] M. Ilyas, I. P. M. Tomlinson, A. Rowan, M. Pignatelli, and W. F. Bodmer "<sup>N</sup><sub>L</sub>-

Catenin mutations in cell lines established from human colorectal cancers”  
*Med. Sci.* 94, (1997) 10330–10334.

- [28] J. M. Mariadason, M. Bordonaro, F. Aslam, L. Shi, M. Kuraguchi, A. Velcich, and L. H. Augenlicht “Down-Regulation of  $\beta$ -Catenin TCF Signaling Is Linked to Colonic Epithelial Cell Differentiation” *Cancer Res.* 61(2001) 3465-3471.
- [29] L. Qi, W. Song, Z. Liu, X. Zhao, W. Cao, and B. Sun “Wnt3a Promotes the Vasculogenic Mimicry Formation of Colon Cancer via Wnt/ $\beta$ -Catenin Signaling” *Int. J. Mol. Sci.* 16 (2015) 18564–18579.
- [30] L. Qi, B. Sun, Z. Liu, R. Cheng, Y. Li, and X. Zhao “Wnt3a expression is associated with epithelial-mesenchymal transition and promotes colon cancer progression.” *J. Exp. Clin. Cancer Res.* 33 (2014) 107.
- [31] A. Panza, V. Pazienza, M. Ripoli, G. Benegiamo, A. Gentile, M. R. Valvano, B. Augello, G. Merla, C. Prattichizzo, F. Tavano, E. Ranieri, P. di Sebastiano, M. Vinciguerra, A. Andriulli, G. Mazzocchi, and A. Piepoli “Interplay between SOX9,  $\beta$ -catenin and PPAR $\gamma$  activation in colorectal cancer” *Biochim. Biophys. Acta - Mol. Cell Res.* 1833 (2013) 1853–1865.
- [32] R. Wang, I.-K. Kwon, M. Thangaraju, N. Singh, K. Liu, P. Jay, F. Hofmann, V. Ganapathy, and D. D. Browning “Type 2 cGMP-dependent protein kinase regulates proliferation and differentiation in the colonic mucosa” *Am. J. Physiol. Gastrointest. Liver Physiol.* 303 (2012) G209-219.
- [33] I.-K. Kwon, R. Wang, M. Thangaraju, H. Shuang, K. Liu, R. Dashwood, N. Dulin, V. Ganapathy, and D. D. Browning “PKG inhibits TCF signaling in colon cancer cells by blocking  $\beta$ -catenin expression and activating FOXO4” *Oncogene* 29 (2010) 3423–3434.

- [34] R. Wang, I.-K. Kwon, M. Hu, and D. D. Browning “Abstract 2583: Regulation of AKT-FoxO signaling by PKG2 inhibits colon cancer cell growth” *Cancer Res.* 73, no. 8 Supplement (2013) 2583–2583.
- [35] A. Bridges, B. Islam, S. Sharman, R. Wang, S. Sridhar, and D. D. Browning “Abstract 1918: Type 2 cGMP-dependent protein kinase activates antineoplastic signaling in the colon” *Cancer Res.* 75, no. 15 Supplement (2015) 1918–1918.

**Fig. 1. Expression of PKG isoforms in the Caco-2, HT-29 and HCT 116 cell lines**

(A) Immunoblotting of total protein extracts from Caco-2, HT-29, HCT 116 colon carcinoma cell lines and SH-SY5Y neuroblastoma cell lines here used as positive control for PKG1 $\alpha$  and PKG1 $\beta$ . Expression of PKG2 could be detected in all cell lines. Lower panels show normalization of the experiments with anti-actin antibodies. (B) Micrographs showing PKG2 cellular localization. Scale bar: 50  $\mu$ m for all panels is shown in the HCT 116 panel.

**Fig. 2. Structures of monomeric and dimeric cGMP analogues displayed in the sodium salt form**

R1+R2 (yellow highlight) resemble the  $\beta$ -phenyl-1,N2-etheno (PET) modification, while R3 (green) refers to the 8-position (C-8) of cGMP and contains either bromine as residue or the linking moiety (including spacer and coupling/bridging functions). Encircled on the left-hand side of the figure we show positions in cGMP that were modified.

**Fig. 3. Phosphorylation of VASP at Serine 239 in the Caco-2, HT-29 and HCT 116 cell lines after treatment with PKG activators**

Phosphorylation of VASP at Serine 239 was analyzed by immunofluorescence in the Caco-2 cell line (A-E), in the HT-29 cell line (F-J) and in the HCT 116 cell line (K-O) after treatment with 8-Br-PET-cGMP at 10  $\mu$ M (B, G, L), compound 1 at 10  $\mu$ M (C, H, M), compound 2 at 10  $\mu$ M (D, I, N) and compound 3 at 10  $\mu$ M (E, J, O) or no treatment (nt) as control (A, F, K). Scale bar: 20  $\mu$ m for all panels is shown in panel O. (P-R) Immunoblotting for pVASP (upper panels) with total protein extracts from Caco-2 (P), HT-29 (Q) and HCT 116 (R) cells, treated with the compounds at 10  $\mu$ M.



Arrows indicate phosphorylated VASP. Loading controls with anti-actin antibodies are shown in the lower panels.

**Fig. 4. Cell viability, cell death and proliferation in the Caco-2 cell line after treatment with cGMP analogues**

(A) Cell viability assay after 24 h of treatment at different concentrations. Values of not treated cells (nt) were set as 100% viability. Symbols for the error bars: 8-Br-PET-cGMP: diamond; compound 1: circle; compound 2: square, compound 3: triangle. (B) Micrographs of DAPI and BrdU staining in not treated cells (nt) and cells treated with compound 2 at 100 nM. Scale bar: 50  $\mu$ m for all panels. (C) Percentages of cell death, as defined by Ethidium Homodimer Assay, were plotted for 8-Br-PET-cGMP and compound 2. (D) Values from the cell viability assay (MTT Assay, grey) and from the proliferation assay (BrdU Assay, black) were plotted as bar graph. (\*  $\leq$  0.05, \*\*  $\leq$  0.01, \*\*\*  $\leq$  0.001)

**Fig. 5. Cell viability, cell death and proliferation in the HT-29 cell line after treatment with cGMP analogues**

(A) Cell viability assay after 24 h of treatment at different concentrations. Values of not treated cells (nt) were set as 100% viability. Symbols for the error bars: 8-Br-PET-cGMP: diamond; compound 1: circle; compound 2: square, compound 3: triangle. (B) Micrographs of DAPI and BrdU staining (upper panels) or DAPI and Ethidium Homodimer staining (EH, lower panels) in not treated cells (nt) and cells treated with compound 1 at 1  $\mu$ M. Scale bar: 50  $\mu$ m for upper panels and 100  $\mu$ m for lower panels. (C) Percentages of cell death, as defined by Ethidium Homodimer Assay, were plotted for 8-Br-PET-cGMP and compound 1. (D) Values from the cell viability

assay (MTT Assay, grey) and from the proliferation assay (BrdU Assay, black) were plotted as bar graph. (\*  $\leq$  0.05, \*\*  $\leq$  0.01, \*\*\*  $\leq$  0.001)

**Fig. 6. Cell viability, cell death and proliferation in the HCT 116 cell line after treatment with cGMP analogues**

(A) Cell viability assay after 24 h of treatment at different concentrations. Values of not treated cells (nt) were set as 100% viability. Symbols for the error bars: 8-Br-PET-cGMP: diamond; compound 1: circle; compound 2: square, compound 3: triangle. (B) Micrographs of DAPI and BrdU staining in not treated cells (nt) and cells treated with compound 2 at 1  $\mu$ M. Scale bar: 50  $\mu$ m for all panels. (C) Percentages of cell death, as defined by Ethidium Homodimer Assay, were plotted for 8-Br-PET-cGMP and compound 2. (D) Values from the cell viability assay (MTT Assay, grey) and from the proliferation assay (BrdU Assay, black) were plotted as bar graph. (\*  $\leq$  0.05, \*\*  $\leq$  0.01, \*\*\*  $\leq$  0.001).

**Fig. 7. Reduced nuclear localization of  $\beta$ -catenin after treatment of the Caco-2 cell line with compound 2**

Confocal images of Caco-2 cells stained with an antibody anti- $\beta$ -catenin. (A) Nuclear localization of  $\beta$ -catenin in not treated Caco-2 cells is indicated by filled arrows in the red channel ( $\beta$ -catenin) image. (B) Reduced nuclear localization of  $\beta$ -catenin could be observed after treatment with 100 nM of compound 2 (empty arrows in the red channel image). Scale bar: 50  $\mu$ m for all panels.

**Fig. 8. Downregulation of PKG2 in the Caco-2 cell line abolishes the effect of compound 2 on cell viability**

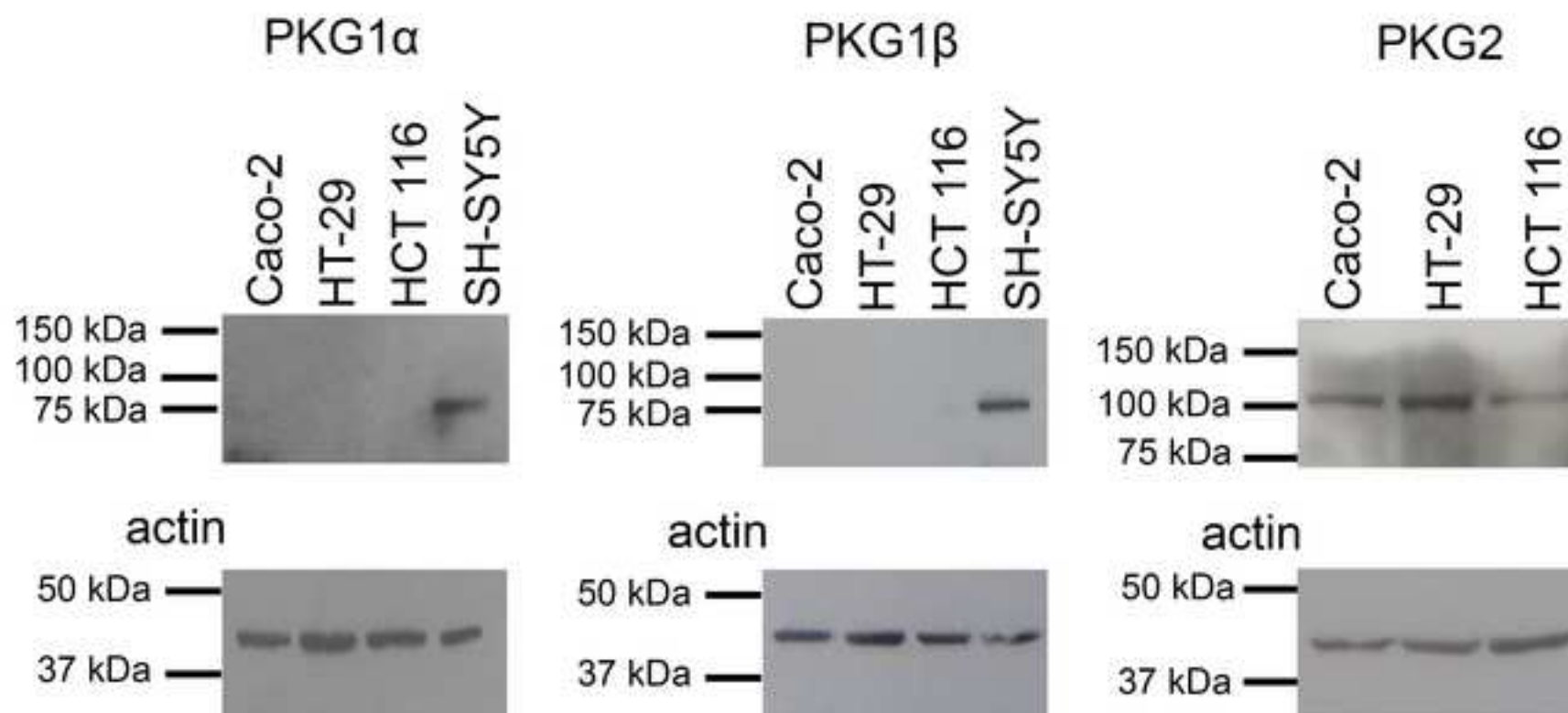
(A) Immunoblotting analyzing expression of PKG2 after treatment with a PKG2 specific shRNA (Caco-2 shRNA) compared to untreated Caco-2 cells (Caco-2) or to Caco-2 cells treated with a negative control scrambled shRNA (Caco-2 scrambled).

(B) Cell viability after 24 h of treatment with compound 2 at different concentrations in Caco-2, Caco-2 scrambled and Caco-2 shRNA PKG2 cells. Value of not treated cells (nt) was set as 100% viability. Symbols for the error bars: Caco-2 = diamond; Caco-2 scrambled = circle; Caco-2 shRNA PKG2 = square. (\*  $\leq 0.05$ , \*\*  $\leq 0.01$ , \*\*\*  $\leq 0.001$ ).

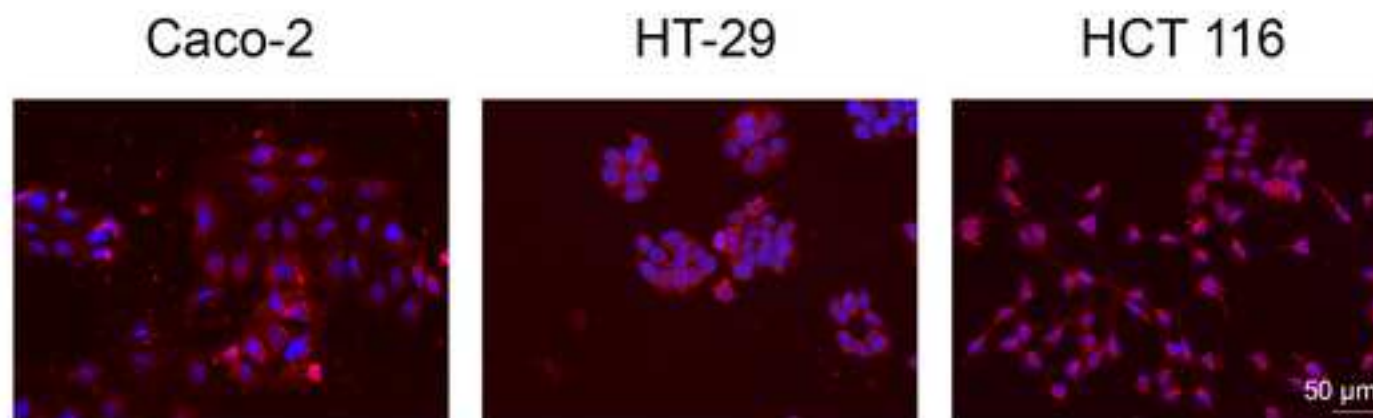
Figure(s)

[Click here to download high resolution image](#)

A

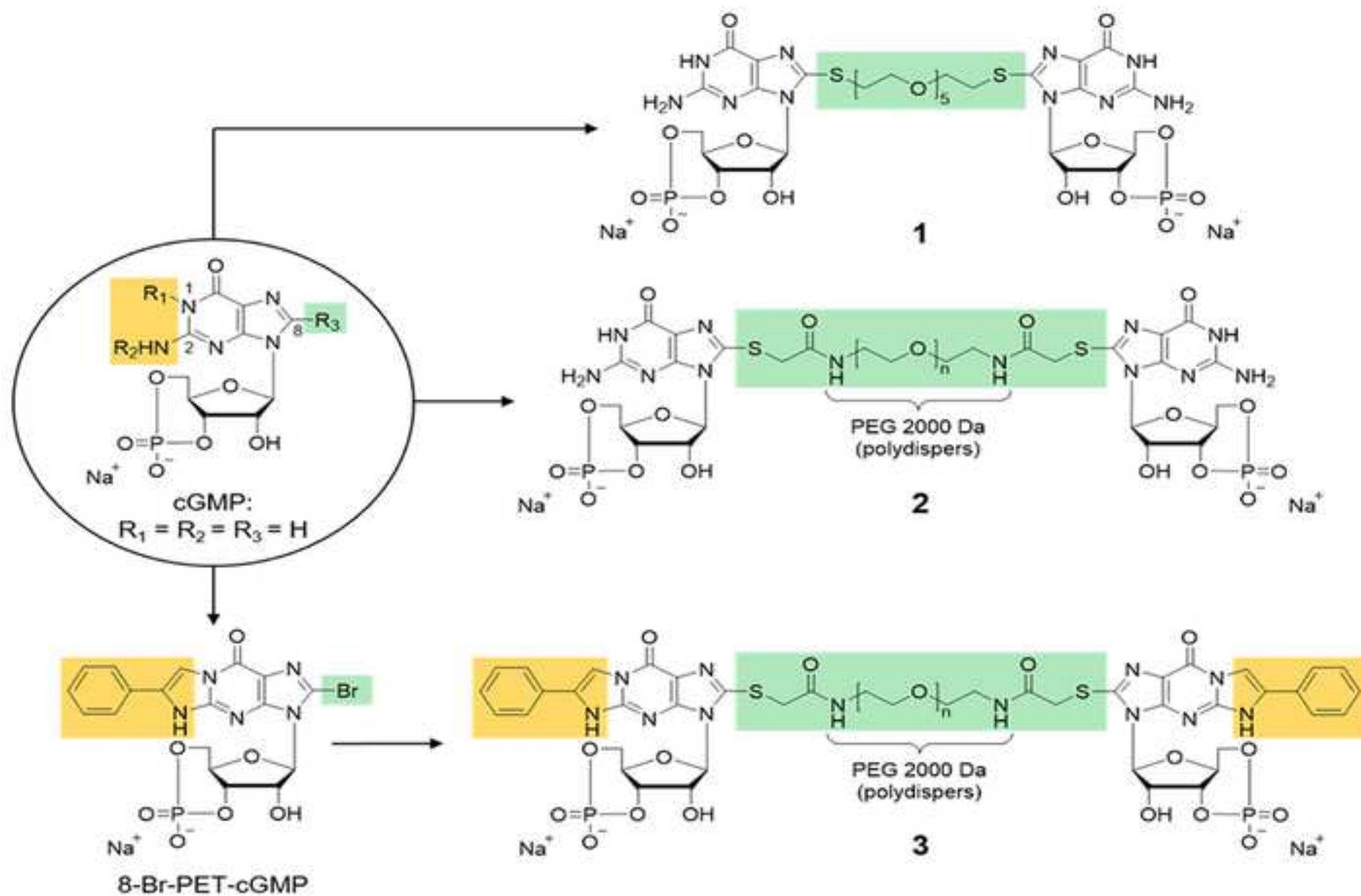


B

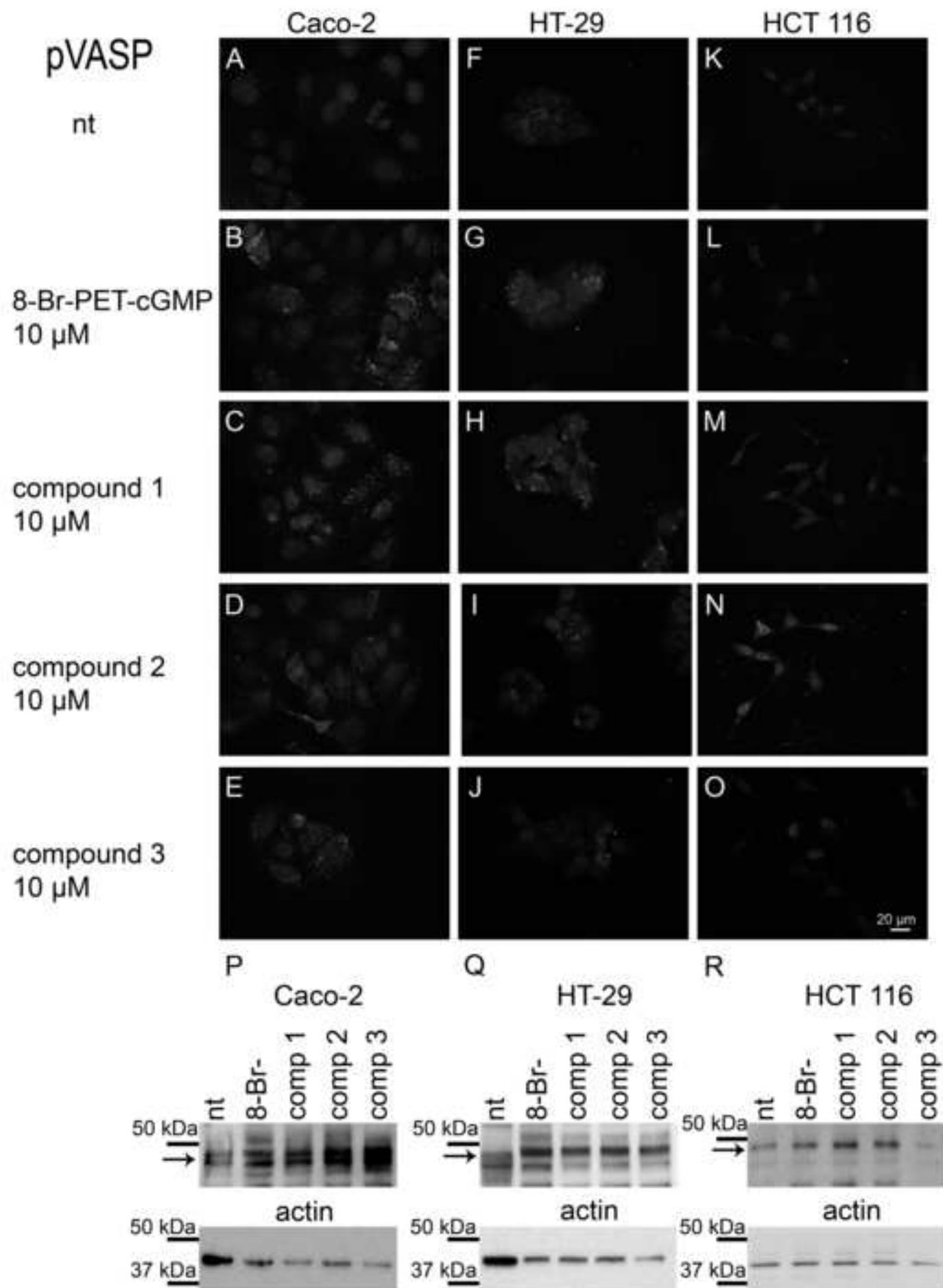


Figure(s)

[Click here to download high resolution image](#)

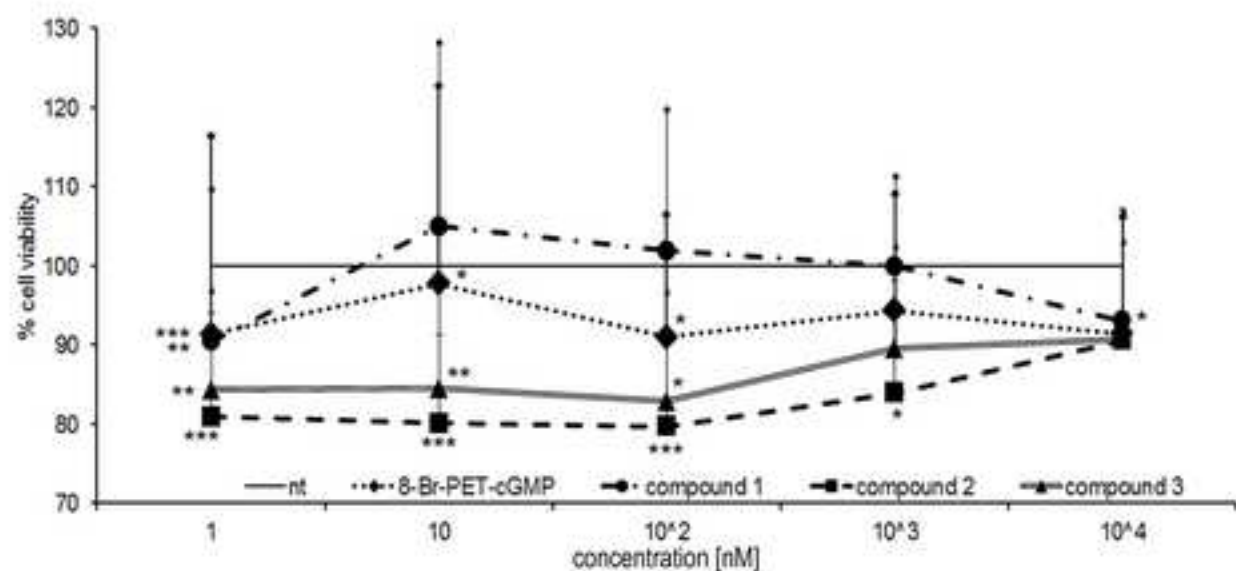


Figure(s)  
[Click here to download high resolution image](#)

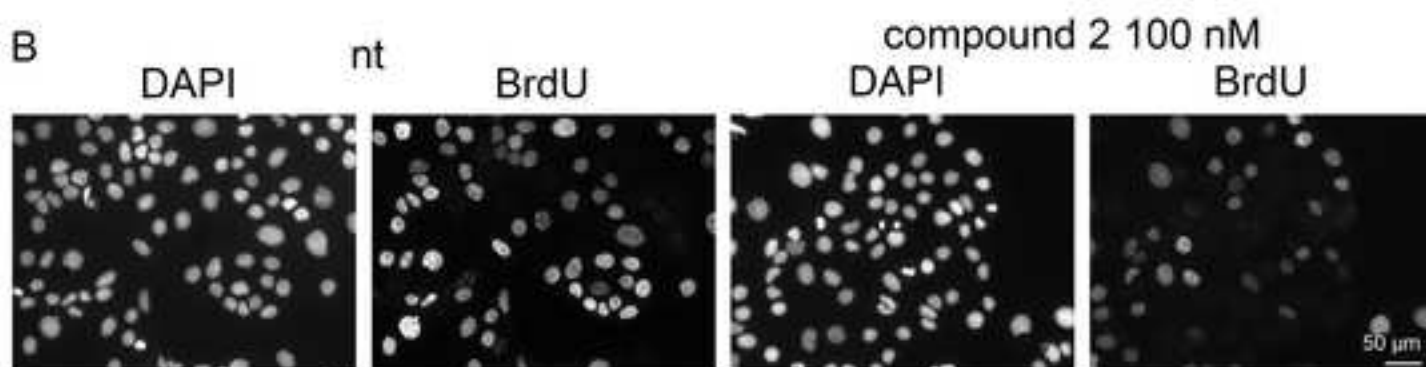


Figure(s)  
[Click here to download high resolution image](#)

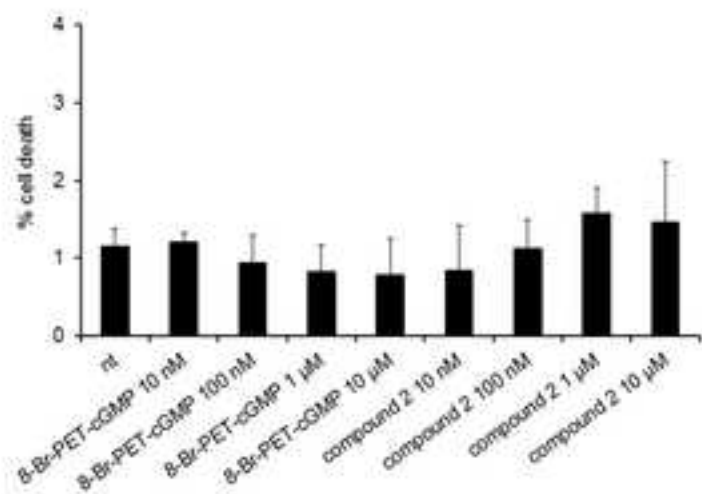
A



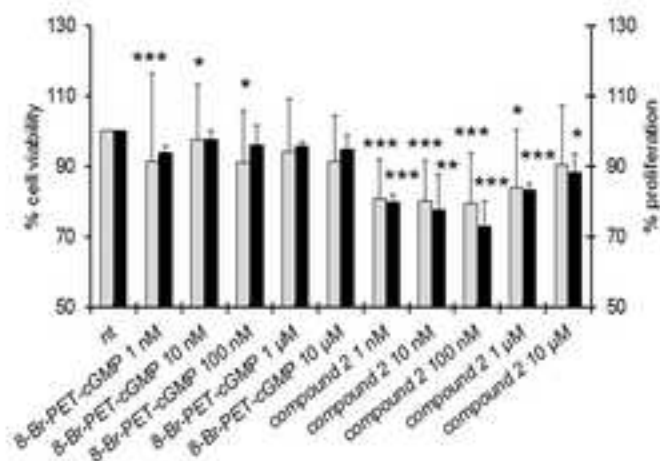
B



C

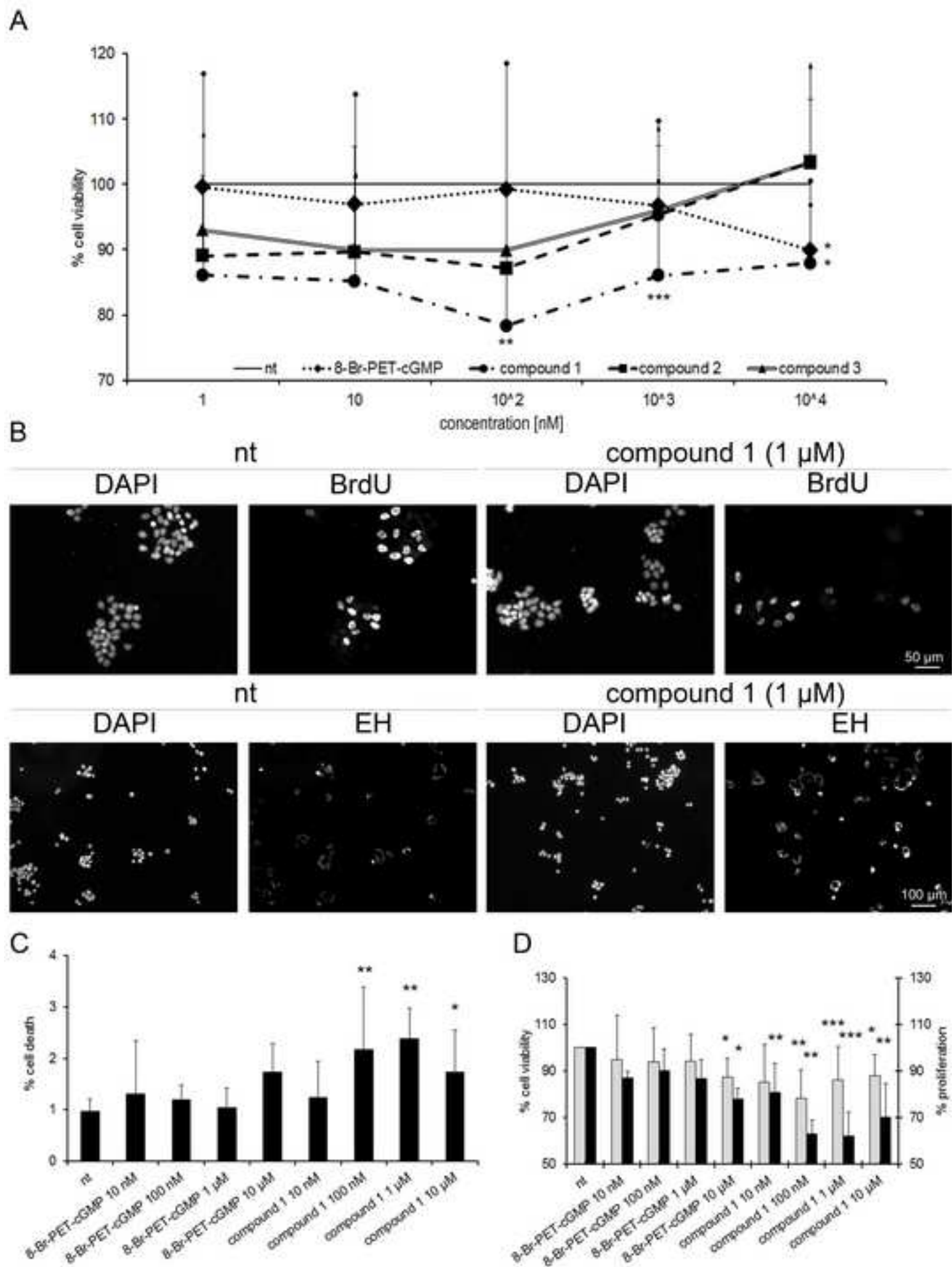


D



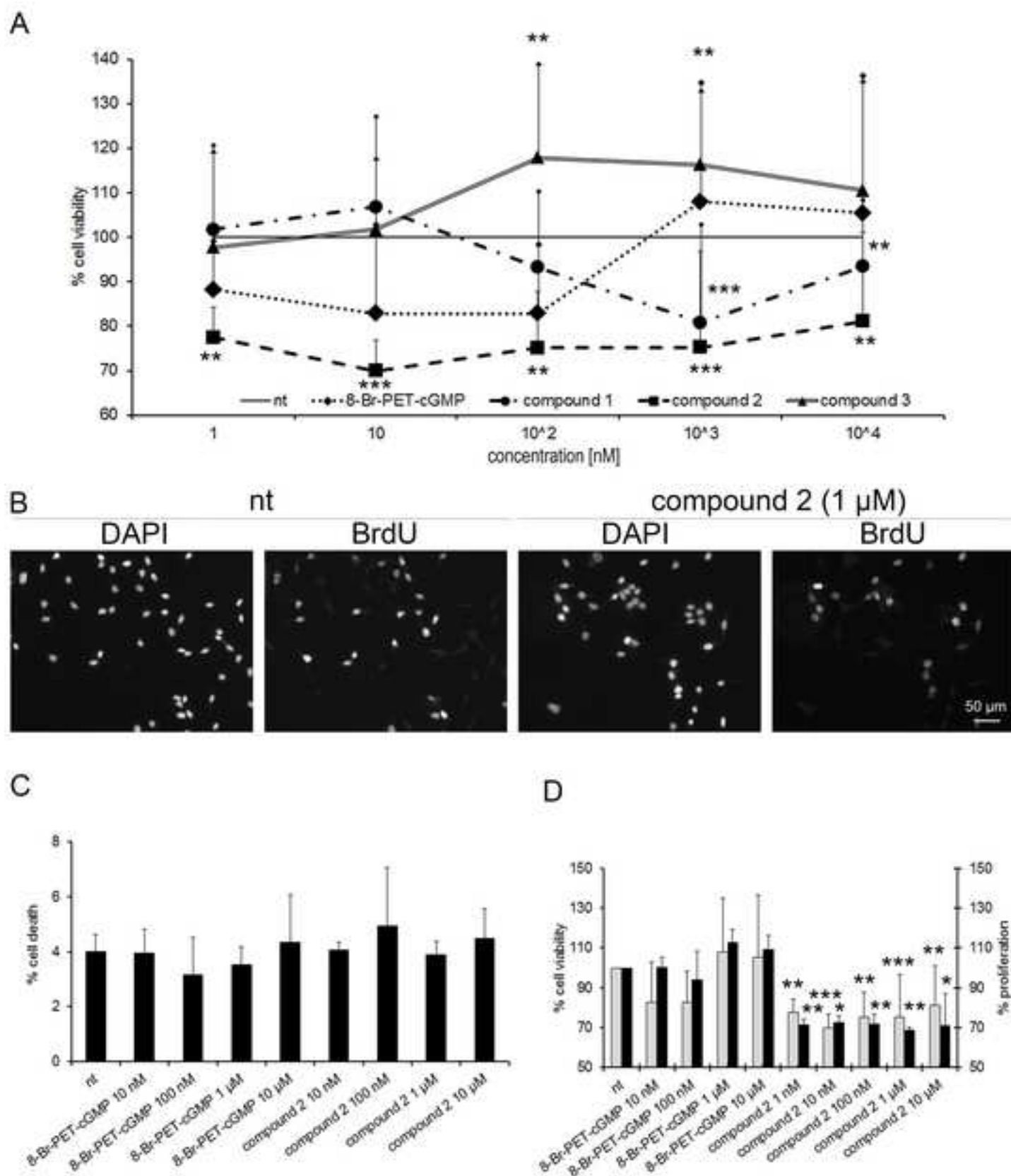


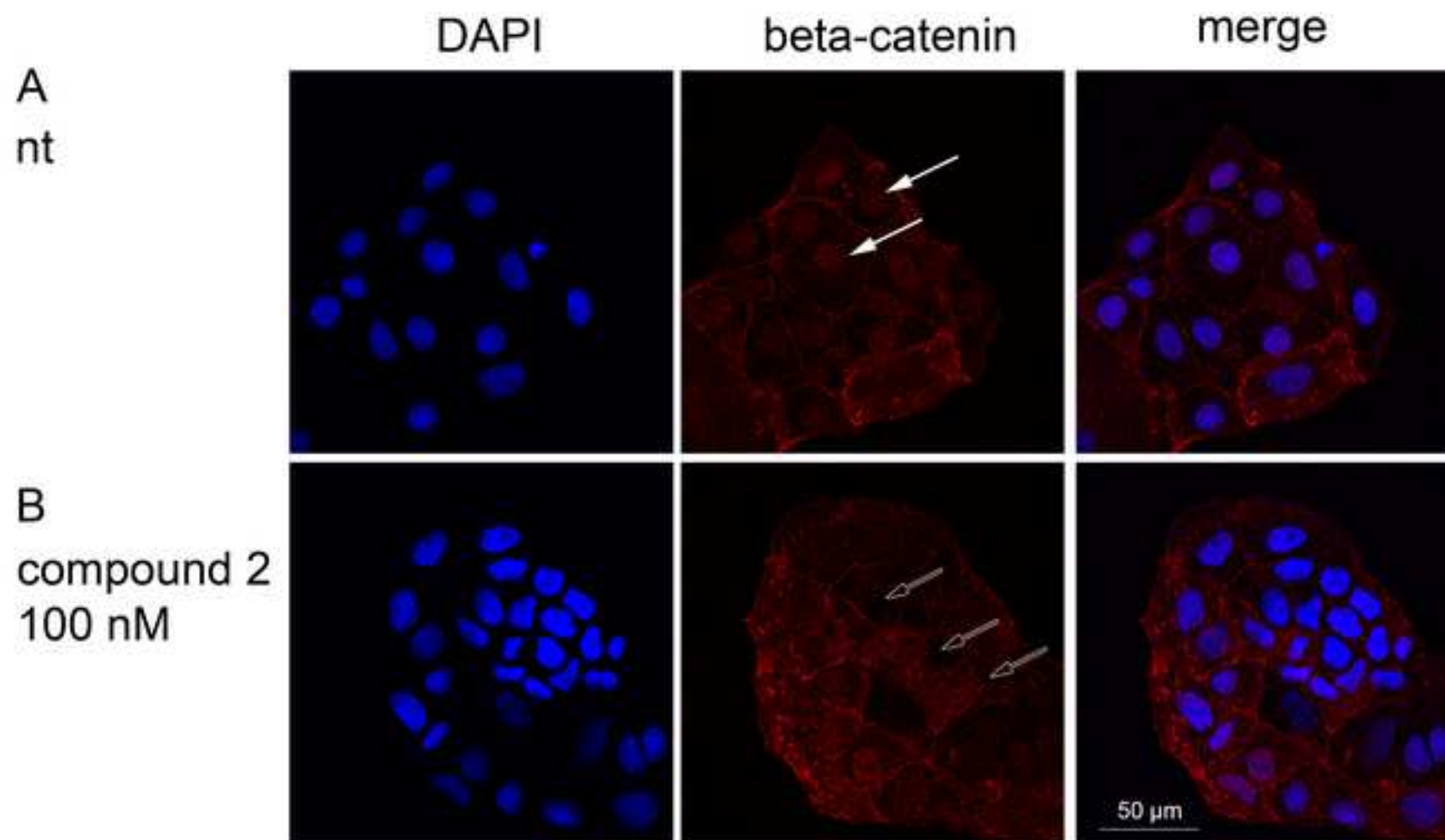
Figure(s)  
[Click here to download high resolution image](#)





Figure(s)  
[Click here to download high resolution image](#)

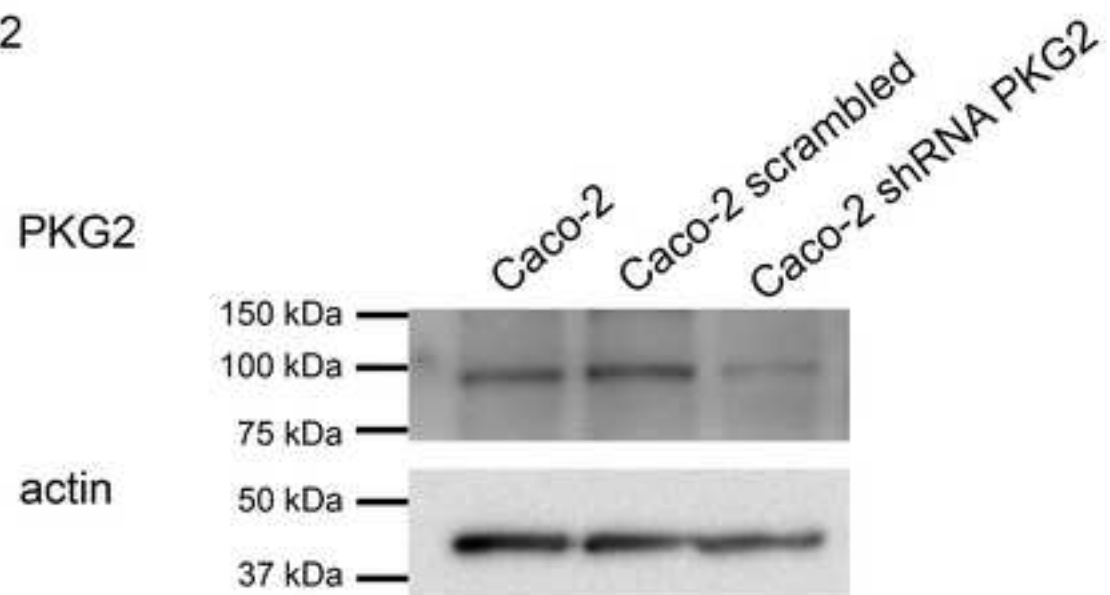




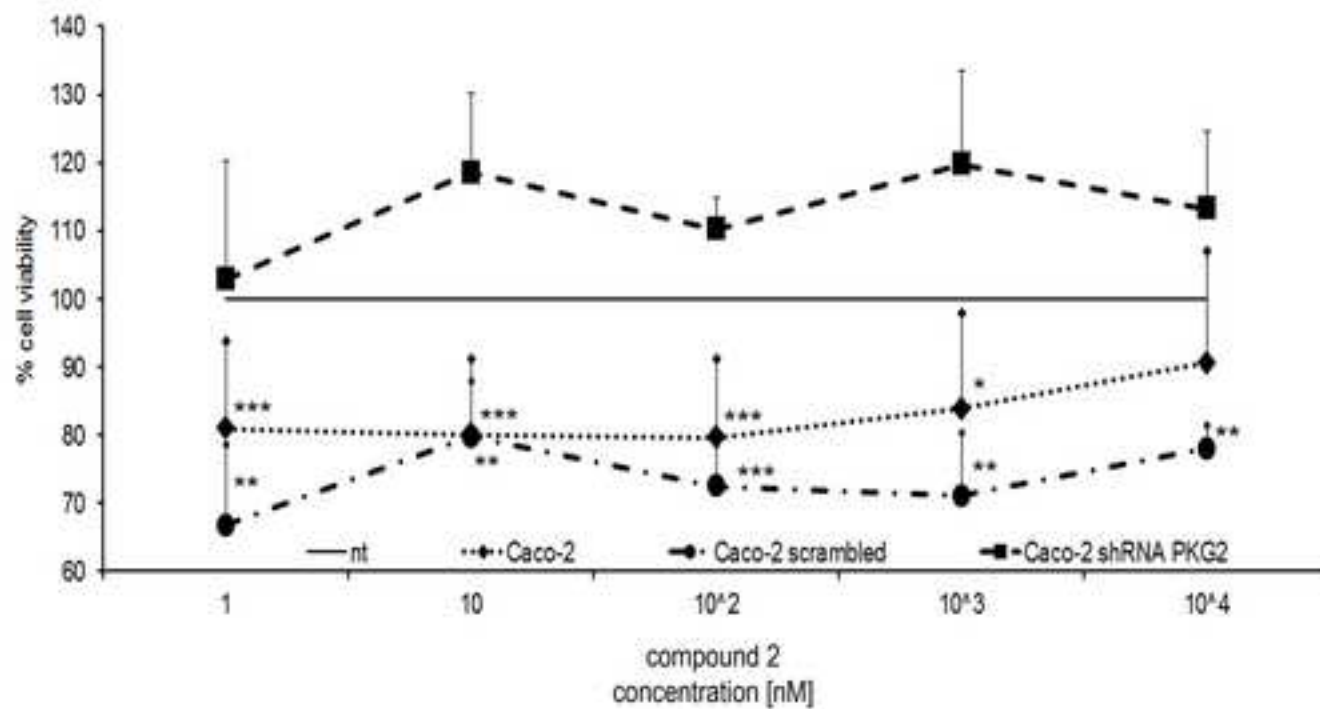
Figure(s)

[Click here to download high resolution image](#)

A Caco-2



B



**Supplementary Material - For Publication Online**

**[Click here to download Supplementary Material - For Publication Online: Suppl methods.docx](#)**